

ACOUSTIC DIFFERENTIAL INTERFERENCE CONTRAST MICROSCOPY

A. Goldstein¹

¹*Department of Applied Physics, Yale University, New Haven, Connecticut 06511, USA*

Conventional Ultrasound can have limited z-resolution and can be characterized by speckle. Differential Interference Contrast Microscopy with light cannot penetrate deep into tissue. Acoustic Differential Interference Contrast Microscopy has the potential to overcome all of these drawbacks, producing non-speckled images and resolving the gradients in the sample with deep-penetrating Ultrasound waves. The potential for this technology will be explored by imaging agarose samples and pig kidneys using a custom-built ultrasound imaging system while focusing the attention on the fundamental characteristics of differential interference contrast microscopy. These include the de-focusing effect as the sample moves out of the focal plane and the three-dimensional effect caused by gradients, leading to bright and dark fringes.

I. INTRODUCTION

Conventional ultrasonic medical imaging is conducted using frequencies between 2 and 20 MHz. Conventional ultrasound technology has gained a niche in the field of prenatal care (obstetric ultrasonography) and it is also practiced in a diverse number of medical applications for diagnoses, therapy, and even surgery with the advantages of being cheaper, safer, more portable, less expensive, and deeper penetrating than other imaging options. However, there are two well-known, fundamental limitations to conventional ultrasound technology. First, it resolves the interfaces between tissue, but not the respective gradients. Detecting interfaces only allows for a two-dimensional image to be formed with limited resolution along the z-axis. Secondly, conventional ultrasound has a high amount of “speckle” noise, a random interference pattern in an image that does not correspond to underlying structure. The presence of speckle in an image has been shown to cause a reduction in contrast resolution as much as a factor of eight, leading to poorer effective resolution of ultrasound compared to Magnetic Resonance Imaging (MRI) and X-Ray technologies.¹

Differential Interference Contrast (DIC) has up until now only effectively been practiced using light waves for applications such as cell culture imaging and test samples with little thickness or amplitude changes. DIC is an imaging method that measures the gradients at the interfaces between tissues.

For example, Figure 1 shows that the positive phase difference at the interface between n_1 and n_2 leads to a bright fringe on the resulting image of a cell. The negative phase difference at the interface between n_2 and n_1 leads to a dark fringe on the resulting image. DIC is characterized by

providing a strong three-dimensional effect and measuring gradients.

However, all of the applications of DIC using light involve imaging at minor depths because light is not anywhere near as effective as ultrasound at penetrating tissue. This inability to penetrate deep into tissue considerably limits the relevant uses of differential interference contrast with light.

Acoustic Differential Interference Contrast combines the deep penetration into tissue that is characteristic of conventional ultrasound technology with the high resolution – non-speckly images – and three-dimensional effect characteristic of differential interference contrast.

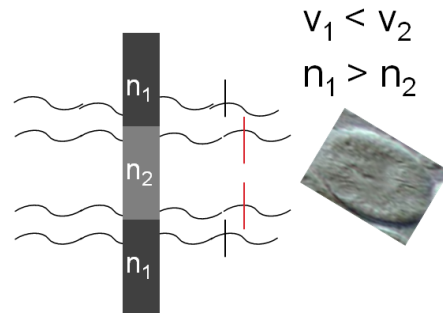


FIG. 1. A diagram showing the basic concept of Differential Interference Contrast Microscopy (DIC).

While there has not been a great deal of previous research done to explore acoustic differential interference contrast, there are a few prior findings that are worth mentioning.

The basic concept of phase contrast imaging was shown to be an effective imaging tool by Farny et al. (2008) for imaging a phantom infused with water columns.² This is effectively the same approach that the following experimental design will use. However, in the case of the following experiment, the phantom agar test sample will only contain one water column through the middle of the agar.

While Farny used a single transducer at a relatively low frequency of 1 MHz, the general physical setup of the detection equipment is a helpful – while, incomplete – model for this experimental setup design.

Li et al. (2005) created an ultrasound phase contrast system to attempt to detect breast cancer lesions and tumors.³ While the results were promising, the low resolution and low signal-to-noise were limiting factors in terms of the extension of this system and the results of their experimentation.

Clement et al. (2004) showed the efficacy of using ultrasound phase contrast imaging to distinguish between fat and tissue when induced by small temperature changes.⁴

II. EXPERIMENTAL DETAILS

A completely original experimental setup was constructed inside a 24" by 24" by 24" glass-walled tank filled with room temperature water. The walls of the tank were covered with echochoic material in order to dampen the reflections of the ultrasound waves off the sides of the tank. The main transmission setup (Figure 2) was submerged inside the water tank and consisted of two identical, focused transducers oriented perpendicular to one another – each with a 1" diameter and a 3" focal length. A two-channel function generator was used to set the voltage received by the two transducers to produce Ultrasound waves of frequencies between 5 and 10 MHz, with the reflected transducer being modulated by an 8.333 Hz (120ms) square wave. The two transducers were separated by a brass beam-splitter that oriented the sound waves parallel to one another before they passed through the test sample.

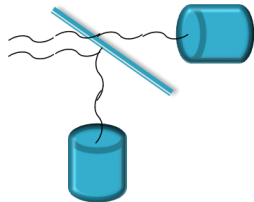


FIG. 2. The transmitted and reflected transducer setup being viewed from above the water tank, looking downwards. The ultrasound waves are animated with curvy lines despite the fact that they have a focusing beam shape.

Two different types of test samples were used during the experimentation. The first was a 3mm thick, donut-shaped agarose gel formed by dissolving 2 percent agarose powder by volume in de-ionized water at near-boiling temperatures. The hot agar was then poured into a 2 inch diameter mount and allowed to cool. A roughly one cm diameter hole was cut out of the 2 percent agarose gel to form the final shape. The second sample was a pig kidney. In order to image a slice of the kidney for a closer look at the structure, a pig kidney was cleaned, sliced at 4 mm thickness, and then vacuum sealed in a thin, rectangular-shaped plastic bag. To image the whole kidney, an unsliced kidney was instead vacuum sealed in a plastic bag for an extended period of time. The plastic bag was then taped to a large, rectangular mount that was attached to an optical post. All kidney test samples were stored at 4°C when not being imaged. Regardless of sample type, the test sample was mounted vertically and controlled by a micrometer in the x-, y-, and z- directions.

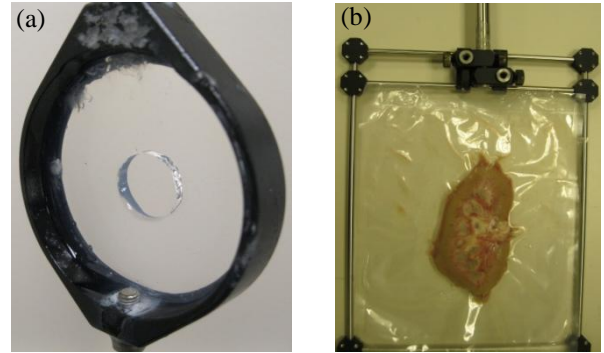


FIG. 3. Examples of the agar (3a) and kidney slice (3b) test samples. The agar is roughly 3 mm thick and the kidney slice is roughly in 4 mm thick. Both of these samples are attached to the motorized, linear translation stages vertically by using the optical post attached to a mounting frame or circle as shown in the figure.

After the sound waves passed through the test sample, the resulting interference pattern was sampled at a point by the hydrophone or with the larger detection area of a separate receiving transducer (depending on the specific stage of the experimental trials). A lock-in amplifier was used to extract the signal that had the exact original frequency of the two transducers. This resulting signal was processed through a simultaneous sampling data acquisition board and converted into an image by custom computer programs in MatLab and LabView. Using two motorized linear stages, the test sample was scanned at a constant speed through the two-dimensional X-Y plane in order to repeatedly collect the signal from the lock-in amplifier at short intervals.

The reason for the two different detection methods that were referenced above (hydrophone and receiving transducer) will become evident in the next section of this paper, but it had much to do with the failure of the initial system to image the unsliced kidney. The effective block diagrams for both of these detection methods are displayed below in Figure 4. It is important to note that the hydrophone detection method included a converging lens to more successfully reflect the relevant signal towards the hydrophone. The ultrasound waves are animated with curvy lines despite the fact that they actually have a focusing beam shape.

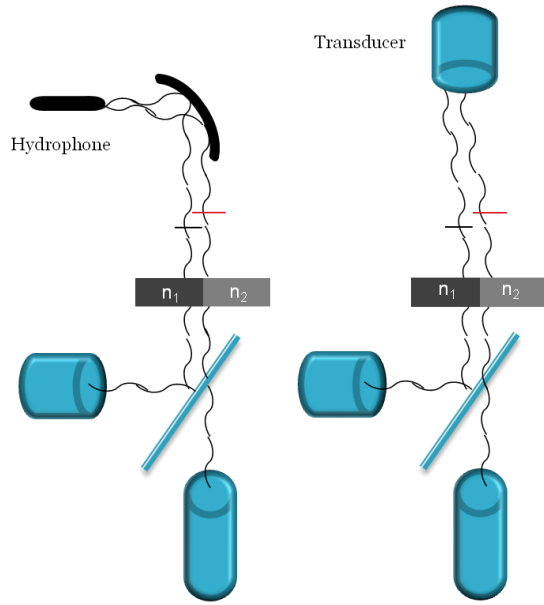


FIG. 4. Side-by-side comparison of the differential interference contrast system with the two different detection methods, via hydrophone and via receiving transducer. The sample is shown as two separate indices of refraction, n_1 and n_2 . The red and black lines in each figure reference the path length difference resulting from this difference in index of refraction.

III. RESULTS

A. Hydrophone Detection System

The effect of film thickness on the characteristic quality of Differential Interference Contrast images is that they will become increasingly less sharp as the test sample is moved out of the focal plane. As is shown on the following page, the clear image in the focal plane (Fig. 5a) is slowly defocused at 5 mm (5b), 10 mm (5c) and 15 mm (5d) away from the focal plane along the z-axis. The disturbance in the upper-right portion of each image is an air bubble, which

defocuses along with the rest of the image as the test sample is moved out of the focal plane. In accordance with the DIC effect, the in-focus image has a similar magnitude of signal outside the agar hole as it does inside of it, with the only stark gradients occurring at the interface between the edge of the agar test sample and the water.

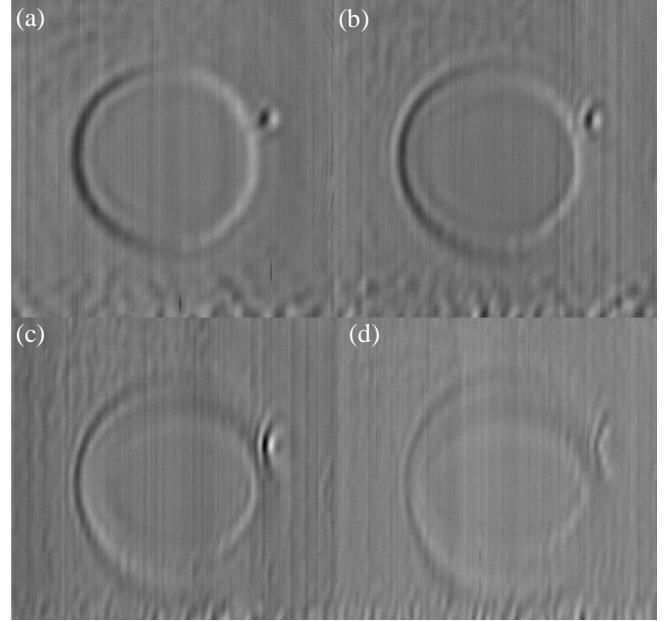


FIG. 5. In-Focus agar test sample image (5a). Through-focus images of the agar test sample at 5 mm (5b), 10 mm (5c) and 15 mm (5d) past the focal plane along the z-axis. All images taken using the hydrophone detection at 5 MHz.

Below is an image of a slice of a kidney taken with the hydrophone at 5 MHz. The reader is able to see the characteristic light and dark fringes at the top and bottom of this image, providing a characteristic, three-dimensional DIC effect.

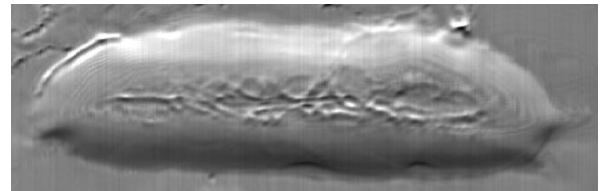


FIG. 6. Acoustic Differential Interference Contrast image of a 4 mm thick slice of a kidney taken using the hydrophone detection at 5 MHz.

It is important to note that the image above is of a slice of a kidney. The next step was to extend the capacity of the system to accommodate unsliced kidneys in order to better mimic the diagnostic value of the acoustic differential interference microscopy design.

Images of the full kidney using the hydrophone assembly at 5MHz (conducted, but not shown in this paper) were too sensitive and did not have the characteristic z-resolution that can be expected of differential interference contrast microscopy partially because of the small detection area of the hydrophone and also due to the attenuation of the signal due to the thickness of a pig kidney, which is generally between 1 and 2 inches thick. In an effort to increase the z-resolution, the frequency was roughly doubled from 5 to 9 MHz to create a four-fold increase in z-resolution (z-resolution is a function of the square of the frequency).

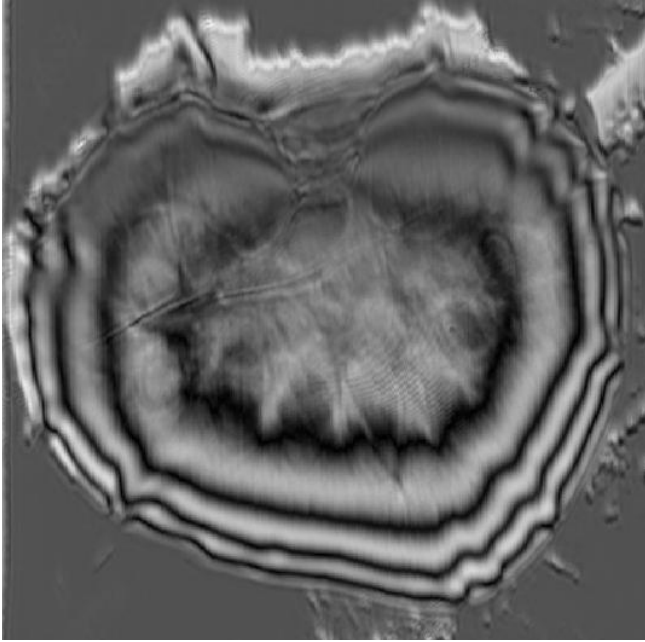


FIG. 7. Acoustic Differential Interference Contrast image of an unsliced kidney taken using the hydrophone detection at 9 MHz.

The previous image (Figure 7) shows a much improved z-resolution with medulla, draining vessels, and a cut along the back of the kidney all visible and reasonably well-defined. However, the ringing around the edges is problematic because it obscures the image.

The ringing effect mainly around the curved edges of the kidney can be attributed to the thin film effect, an artifact of the method in which the kidney was encased in the plastic vacuum sealed bag. The sheer thickness of the kidney caused the vacuum sealing process to warp the

plastic bag tight against the curved sides of the kidney. The thin film effect occurs if $2t$ – two times the thickness of the thin plastic vacuum bag – is on the order of $\lambda/2$ where λ is the corresponding wavelength associated with the frequency of the waves emitted from the transducers. At a 5MHz frequency, the wavelength is long enough so that $2t$ is still sufficiently small and the thin film effect is not observed. However, at a 9MHz frequency, the wavelength is considerably shorter and $2t$ is no longer negligible. For a thick kidney, the curved edges curve the interfaces – Figure 8 below applying the thin-film effect to the bag-kidney system presupposes that the interfaces will be linear – which leads to the system being sensitive along the curved sections, creating bright and dark fringes as shown in Figure 7.

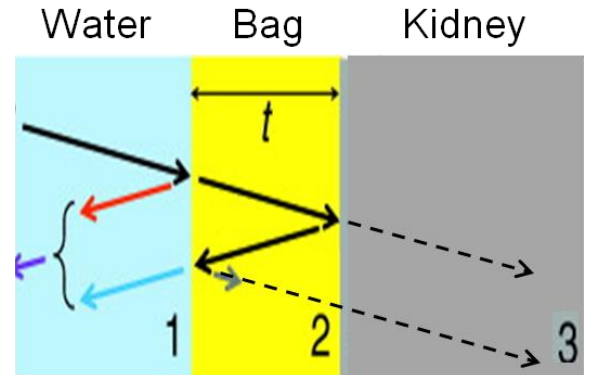


FIG. 8. The thin-film effect as applied to the bag-kidney system. The thickness of the bag t becomes on the order of the wavelength $\lambda/2$ when the frequency is increased from 5 MHz to 9 MHz.

B. Receiving Transducer Detection System

The complicating factors involving the thin-film effect necessitated the shift towards a receiving transducer setup with a larger detection area. It became evident that the ultrasound waves were refracting ever so slightly after passing through the test sample, creating a scenario where one of the transducer beams is amplified with respect to the other.

This wider (roughly 1 inch) detection area will help to nullify the effect of the sound waves refracting by narrow amounts due to deviations in the sample. The goal of this approach is to produce a sound profile that will provide the necessary contrast. The basic idea is that for the hydrophone (smaller detection area), a slight shift of the interference pattern doesn't change the area under the curve: the voltage. However, for a larger detection area such as a transducer, a similar slight shift of the interference pattern does change the area under the curve, providing the necessary contrast.

The interference pattern can be translated by shifting one of the transducers relative to the other.

Figure 9 is analogous to Figure 5a (and Figure 11a) in that it is an image of an agar test sample in the focal plane. Figure 9 looks slightly less focused given that it was smoothed using a custom normalization program to reduce the “striping” effects of the scanning process. The reader can observe that the transducer detection system produces images of a similar quality to the hydrophone detection system.

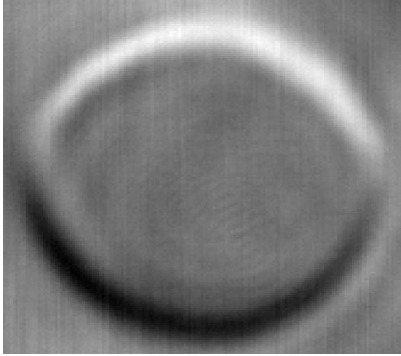


FIG. 9. In-Focus agar test sample image normalized to reduce “striping” effect. Image taken using the transducer detection at 5 MHz.

The transducer detection system was then applied to image an unsliced kidney at a frequency of 5 MHz. Figure 10 shows the improved z-resolution of Figure 7 without the ringing effect to obscure the image. Once again, the medulla, draining vessels, and other structures are visible and reasonably well-defined. It is important to keep in mind that comparable z-resolution was achieved at about half the frequency of Figure 7, which would imply that the z-resolution could only improve at somewhat higher frequencies.

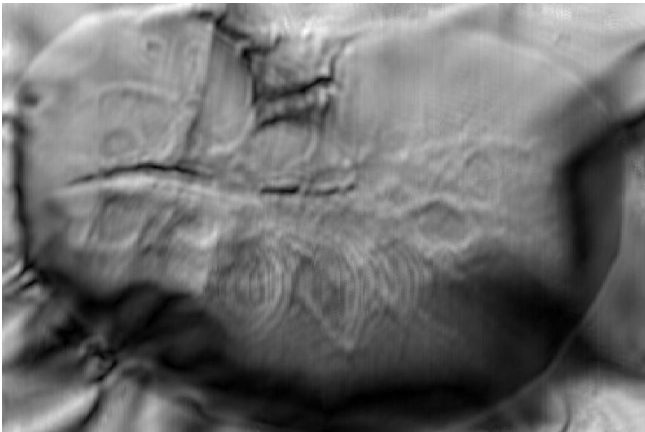


FIG. 10. Acoustic Differential Interference Contrast image of a whole kidney taken with transducer detection system at 5 MHz.

Therefore, the next logical step in this experimental process was to increase the frequency from 5 MHz to 10 MHz and assess the increase in resolution. The resulting images are displayed in Figure 11 below with the most well-defined image in the focal plane (Fig. 11a) slowly defocusing at 2.5 mm (11b), 7.5 mm (11c) and 12.5 mm (11d) away from the focal plane along the z-axis. Figure 11c and 11d are different in that Figure 11d begins to become distorted. The consistent disturbances in the upper right and lower left hand corners of each image are artifacts of the sample and not particularly relevant to the assessment of the z-resolution of the system at 10MHz.

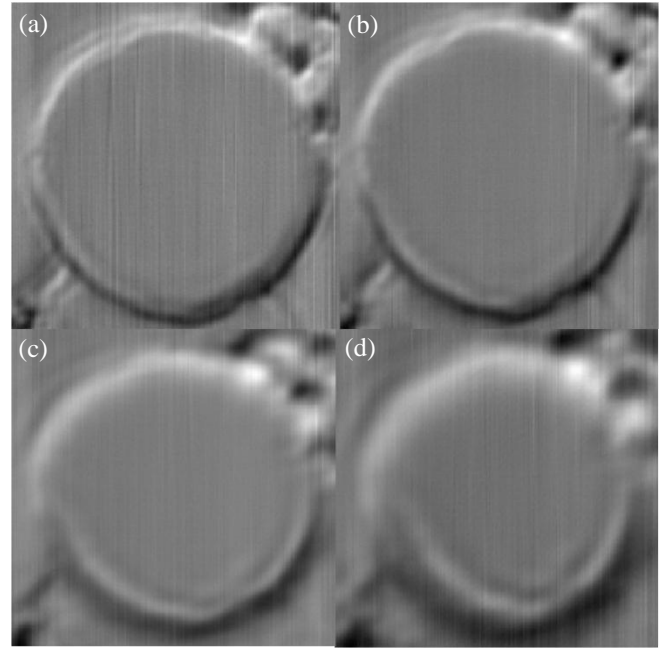


FIG. 11. In-Focus agar test sample image (11a). Through-focus of the agar test sample at 2.5 mm (11b), 7.5 mm (11c) and 12.5 mm (11d) past the focal plane along the z-axis. All images taken using the transducer detection at 10 MHz.

IV. DISCUSSION

The two different detection methods had different advantages and disadvantages, but the fact that both were used to create fully-functioning acoustic differential interference contrast systems provides more validity to the results. In other words, the size of the detection area and method of sampling from the resulting interference patterns did not have an impact on the fundamental image results.

Increasing the frequency to 10MHz made the system much more sensitive to small perturbations and made the alignment somewhat more challenging, but it allowed for a sharper contrast along the interfaces between tissues. This is

exemplified by the sharp nature of the change in the differential interference contrast signal in Figure 11a when compared with Figure 9 or Figure 5a. By eye, it appears that the width of the gradient in Figure 11a is many times narrower than the analogous width of Figure 9 or of Figure 5a.

There were a number of limitations that affected this experiment and the experimental setup in general. The sensitivity of most components and elements of the experimental setup led to extremely noisy signals from time-to-time that the lock-in amplifier was not able to completely account for. There were concerns about consistency of the results from week to week with minor shifts in alignment, and of the two transducers' effective strength relative to one another. A final limitation was the large amount of time required to collect the data for each image. There is an incredibly high resolution possible with this system, but it also requires a great deal of time per image to realize this resolution potential.

V. CONCLUSIONS

In summary, the results from the experimental systems showed that differential interference contrast microscopy can work with light as well as sound in transmission through a tissue sample. The strong similarities between light and acoustic differential interference contrast microscopy are

evident in the similarities regarding the de-focusing effect as the sample is moved out of the focal plane, the bright and the dark fringes leading to a three-dimensional effect, the emphasis on resolving gradients between tissues as opposed to the interfaces between tissues.

Further work would certainly include a scan of an unsliced pig kidney at 10 MHz with the transducer detection system. This would allow for the verification of the preliminary findings of Figure 11: large frequencies lead to sharper gradients. The ultimate translation of this technology to medical diagnostic imaging could be realized with applications to breast cancer or skin cancer, but this would require an extension of the current system towards a two-dimensional phased array.

ACKNOWLEDGEMENTS

I would like to acknowledge the support, mentorship, research collaboration, and camaraderie of Principal Investigator and Biomedical Engineering Professor, Michael Levene: my research advisor and an excellent friend. Additionally, I would like to acknowledge the first-class advice and wisdom of my academic advisor and Applied Physics Director of Undergraduate Studies, Professor Victor Henrich.

¹ Bamber, J, and C Daft. "Adaptive Filtering For Reduction Of Speckle In Ultrasonic Pulse-echo Images." *Ultrasonics* 24.1 (1986): 41-44. Print.

² Farny, Caleb H., and Greg T. Clement. "Feasibility Of Ultrasound Phase Contrast For Heating Localization." *The Journal of the Acoustical Society of America* 123.3 (2008): 1773. Print.

³ Li, Cuiping, Nebojsa Duric, Peter Littrup, and Lianjie Huang. "In Vivo Breast Sound-Speed Imaging With Ultrasound Tomography." *Ultrasound in Medicine & Biology* 35.10 (2009): 1615-1628. Print.

⁴ Clement, G T, and K Hynynen. "Ultrasound Phase-contrast Transmission Imaging Of Localized Thermal Variation And The Identification Of Fat/tissue Boundaries." *Physics in Medicine and Biology* 50.7 (2005): 1585-1600. Print.